Fully 3D Iterative Reconstruction of Planogram Data

P. E. Kinahan[1], D. Brasse[1], M. Defrise[2], R. Clackdoyle[3], C. Comtat[4], C. Michel[5], X Liu[2]

[1]*Department of Radiology, University of Pittsburgh, Pittsburgh, PA 15213 USA*

[2]*Department of Medical Research, SHFJ, CEA, 91401 Orsay, France*

[3]*Department of Radiology, University of Utah, Salt Lake City, UT 84108 USA*

[4]*Division of Nuclear Medicine, University Hospital AZ-VUB, B-1090, Belgium*

[5]*CTI Inc., Knoxville, TN USA*

Background

At the previous Fully 3D meeting we presented the concept of the 'planogram' data format for fully-3D imaging. The planogram data format is a generalization of the 2D linogram data format of Edholm et al. [1, 2]. This planogram format is based on the native acquisition geometry of planar detectors, illustrated in figure 1, where the natural rectangular detector coordinates are given by (x_{d1}, y_{d1}) and (x_{d2}, y_{d2}) for two individual detector events that determine a line of response (LOR).

We can parameterize the LOR orientation by the coordinates (u_1, u_2, v_1, v_2) where $u_1 = (x_{d1} - x_{d2})/2$, $u_2 = (y_{d1} + y_{d2})/2$, $v_1 = -(x_{d1} + x_{d2})/2$, and $v_2 = (y_{d2} - y_{d1})/2$. In this parameterization we assume the detectors are separated by unit distance so (v_1, v_2) are the tangents of the angle of the LOR projected onto the $x-y$ and $y-z$ planes, respectively relative to the y axis. We can then further parameterize the LOR w.r.t. the y-coordinate as $u_1 = x + v_1 y$ and $u_2 = z + v_2 y$.

If we regard a fixed (x, y, z), then the subset of LORs passing through that point will appear as a 2D plane in the (u_1, u_2, v_1, v_2)-space, thus the choice of the term 'planogram' for the data acquisition histogram.

In this case the measured line integral data are defined, after appropriate scaling by $((1 + v_1^2 + v_2^2)^{-1/2})$ (determined by the angle between the detector surface and the unit normal vector), as:

$$g_1(u_1, u_2, v_1, v_2) = \int_{-\infty}^{\infty} f(x, y, z)\,\mathrm{d}y = \int_{-1/2}^{1/2} f(u_1 - v_1 y, y, u_2 - v_2 y)\,\mathrm{d}y \quad (1)$$

where we now use $x = u_1 - v_1 y$ and $z = u_2 - v_2 y$. We can also define backprojection as:

$$b_1(x, y, z) = \int_{-\infty}^{\infty}\int_{-\infty}^{\infty} g_1(x + v_1 y, z + v_2 y, v_1, v_2)\,dv_1 dv_2 \quad (2)$$

To adequately sample the function $f(x, y, z)$, we assume the data has been collected from a second detector position rotated about the z-axis by 90 deg, so that $u_1 = y - v_1 x$ and $u_2 = z - v_2 x$.

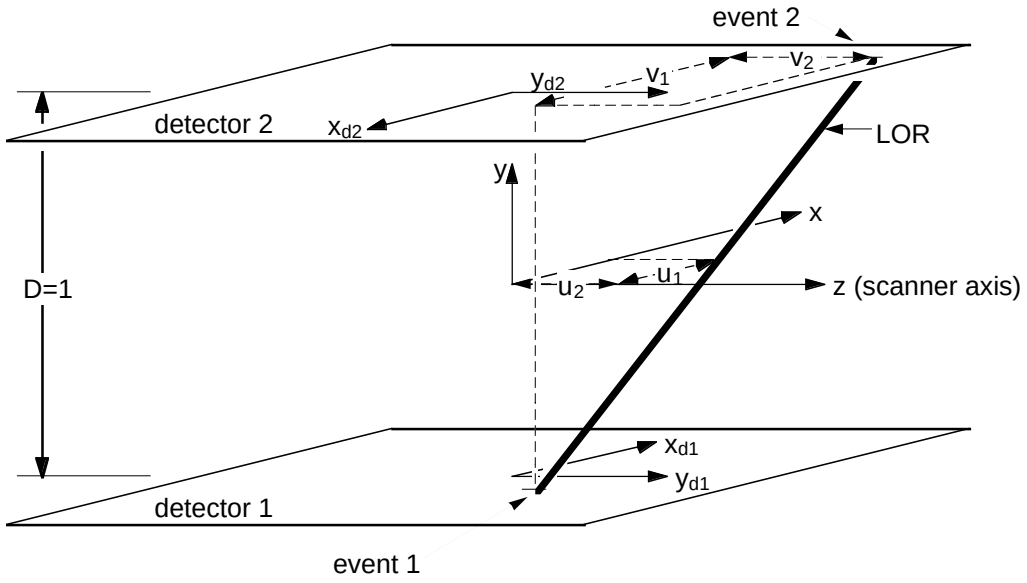

Figure 1. Coordinates used to index a LOR between two detector elements on planar detectors.

This work is supported by NIH grant CA80943.

Then by symmetry we have:

$$g_2(u_1,u_2,v_1,v_2) = \int_{-\infty}^{\infty} f(x,y,z)\,\mathrm{d}x = \int_{-1/2}^{1/2} f(x,u_1+v_1x,u_2+v_2x)\,\mathrm{d}x \quad (3)$$

where now $y = u_1 + v_1 x$ and $z = u_2 + v_2 x$. For this position we define backprojection as:

$$b_2(x,y,z) = \int_{-\infty}^{\infty}\int_{-\infty}^{\infty} g_2(y - v_1x, z - v_2x, v_1, v_2)\,dv_1 dv_2 \quad (4)$$

Two key properties of the planogram data formats are based on Fourier transform relations. We define:

$$G_{1,1111}(U_1,U_2,V_1,V_2) = \int_{-\infty}^{\infty}\int_{-\infty}^{\infty}\int_{-\infty}^{\infty}\int_{-\infty}^{\infty} g_1(u_1,u_2,v_1,v_2) \cdot \mathrm{e}^{-2\mathrm{i}\pi(u_1U_1+u_2U_2+v_1V_1+v_2V_2)}\,\mathrm{d}u_1\mathrm{d}u_2\mathrm{d}v_1\mathrm{d}v_2 \quad (5)$$

and

$$B_{1,101}(X,y,Z) = \int_{-\infty}^{\infty}\int_{-\infty}^{\infty} b_1(x,y,z)\mathrm{e}^{-2\mathrm{i}\pi(x\mathrm{X}+z\mathrm{Z})}\,\mathrm{d}x\mathrm{d}z \quad (6)$$

where the subscript indicates w.r.t. which variable the Fourier transform has been taken.

The quadruple integral in equation (5) is over the (u_1,u_2,v_1,v_2) domain covered by the pair of rectangular detectors. The limits are implicitly extended to the whole of $\mathcal{R}^4$. Substituting equation (2) into equation (6), and by symmetry for equation (4), we have the surprising results that,

$$B_{1,101}(X,y,Z) = G_{1,1111}(X,Z,-yX,-yZ) \quad (7a)$$

and

$$B_{2,011}(x,Y,Z) = G_{2,1111}(Y,Z,xY,xZ) \quad (7b)$$

The results are a case of the 4D version of the central section theorem. Equation (7) indicates that fully 3D backprojection can be performed with only using Fourier transform operations. An algorithm for analytic backprojection is:

1. Compute the 4D Fourier transform $G_{1,1111}(U_1,U_2,V_1,V_2)$.
2. For each y_i:
   - interpolate $B_{1,101}(X,y_i,Z)$ using equation (7a).
   - compute the inverse 2D Fourier transform to obtain $b_1(x,y_i,z)$.
3. Repeat step 2 for $G_{2,1111}(U_1,U_2,V_1,V_2)$, using each x_i to interpolate $B_{2,011}(x_i,Y,Z)$ using equation (7b).

We have presented results showing that this backprojection method offers speed improvements of approximately 15 compared to standard fully 3D sinogram methods [3]. These speed improvements can be further leveraged by the use of readily available FFT processors.

Application to iterative reconstruction methods

To investigate the application of this approach to iterative methods we make two observations:

1. Equation (7) (backprojection) does not require that the data are non-truncated.
2. If we compute the 2D Fourier transform of equation (1), we derive a version of the 3D central section theorem:

$$G_{1,1100}(U_1,U_2,v_1,v_2) = F(U_1,v_1U_1+v_2U_2,U_2) \quad (8)$$

with a similar version for $G_{2,1100}(U_1,U_2,v_1,v_2)$.

Equation (8) implies a fast method for forward-projection, so from equations (7) and (8) we thus have methods for fast forward-projection and backprojection. These are suitable for incorporation into the 3D-OSEM algorithm [4, 5], represented here in two steps:

$$g_i^{(k)} = \sum_{j'} a_{ij'} f_{j'}^{(k)}$$
$$f_j^{(k+1)} = \frac{f_j^{(k)}}{\sum_{i\in S_N} a_{ij}} \left\{ \sum_{i\in S_N} a_{ij} \frac{g_i}{g_i^{(k)}} \right\} \quad (9)$$

where $f_j^{(k)}$ is the k-th estimate of the value of image voxel j, g_i is the measured data in planogram bin i, and $g_i^{(k)}$ is the k-th estimate of the value of image voxel j. The probability of an event from image voxel j being detected in planogram bin i is given by a_{ij} using those LORs comprising the data subset S_N [6]. The first part of equation (9) can be regarded as a forward-projection, which can be computed with equation (8). Typically unmeasured (truncated) data are also estimated, which can be discarded. The portion within braces of the second part of equation (9) can be regarded as the backprojection of the ratio of the measured/estimated data. This can be computed using equation (7). We note that this approach corresponds to using a line integral model of the a_{ij}, and that using equations (7) and (8) does not strictly correspond to the same a_{ij} due to numerical discretization errors, that is we are using un-matched backprojector/forward projector pairs.

Implementation

The accuracy of using equation (8) for forward-projection is illustrated in figure 2.

The version of 3D-OSEM described by equation (9) was implemented using equations (7) and (8) for backprojection and forward-projection. The use of two detector positions leads to a simple sorting of the data into two subsets. The results of this approach are illustrated in figure 3. We note that the use of only two subsets is not an optimal implementation as figure 3 that 16 iterations are required to reach a minimum RMS error estimate.

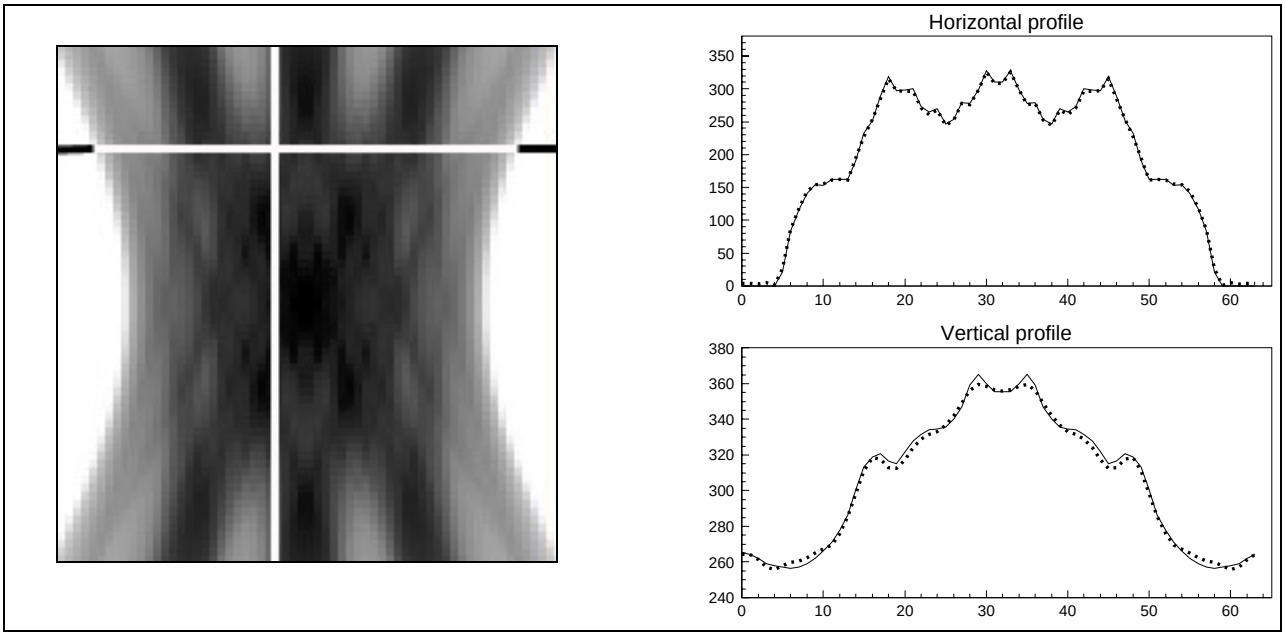

Figure 2. Forward projection planogram data using equation (9). Solid lines in the image indicate the positions of the profiles shown on the right for the Forward projected data (dotted line) compared to the original simulated planogram data (solid line).

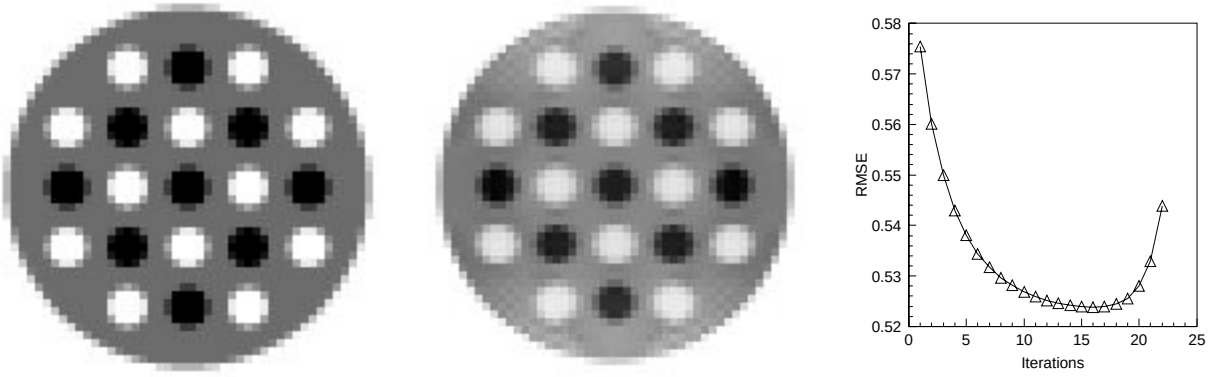

Transverse section of original object

Estimated object after 16 iterations

RMS error between original object and estimated object at each iteration

Figure 3. 3D-OSEM method applied to a noiseless spherical object with imbedded hot and cold spheres for two subsets with up to 20 iterations.

This approach can be used for any iterative method using repeated 3D backprojection and forward-projection. We will present further results on the relative timing of this approach for iterative 3D reconstruction methods as well as the performance in the presence of statistical noise and with increasing numbers of subsets.

References

[1] Edholm PR and Herman GT, "Linograms in Image Reconstruction from Projections," *IEEE Trans Med Imag*, Vol. MI-6, pp. 301-307, 1987.

[2] Magnusson M, "Linogram and Other Direct methods for Tomographic Reconstuction," Ph.D. Thesis, Linköping University, Linköping, Sweden, 1993.

[3] Brasse D, et al., "Fast Fully 3D Image Reconstruction Using Planograms," Proceedings of: IEEE Nuclear Science Symposium and Medical Imaging Conference, Lyon, France, 2000, pp.

[4] Johnson CA, et al, "Evaluation of 3D reconstruction algorithms for a small animal PET scanner," *IEEE Trans Nuc Sci*, Vol. 44, pp. 1303-1308, 1997.

[5] Liu X, et al. "Comparison of 3D reconstruction with 3D-OSEM and with FORE+OSEM for PET," *IEEE Trans Med Imag*, Vol. , pp. (to appear), 2001.

[6] Hudson H and Larkin R, "Accelerated image reconstruction using ordered subsets of projection data," *IEEE Trans Med Imag*, Vol. 13, pp. 601-609, 1994.